FLOW STRUCTURE FORMATION IN HIGH-VELOCITY GAS-FLUIDIZED BEDS

Jie Li and J. A. M. Kuipers

Department of Chemical Engineering
University of Twente,
7500AE, Enschede, The Netherlands

Abstract --- The occurrence of heterogeneous flow structures in gas-particle flows seriously affects the gas–solid contacting and transport processes in high-velocity fluidized beds. A computational study, using a discrete particle method based on Molecular Dynamics techniques, has been carried out to explore the mechanisms underlying the cluster and the core/annulus structure formation. Based on energy budget analysis including work done by the drag force, kinetic energy, rotational energy, potential energy, and energy dissipation due to particle-particle and particle-wall collisions, the role of 1) gas-solid interaction and 2) inelastic collisions between the particles are elucidated. It is concluded that the competition between gas-solid interaction and particle-particle interaction determines the pattern formation in high-velocity gas-solid flows: if the gas-solid interaction (drag) dominates, a uniform flow structure prevails. Otherwise, a heterogeneous pattern exists, which could be induced by both particle-particle collisions and gas-solid interaction. Although both factors could cause the flow instability, the drag force is demonstrated to be the necessary condition to trigger the heterogeneous flow structure formation.

Introduction

The occurrence of heterogeneous flow structures in gas-particle flows seriously affects the quality of gas–solid contacting and transport processes in high velocity fluidized beds. Therefore, it has attracted interest from both academic and industrial researchers. In the last decade, great efforts have been made to understand this heterogeneous structure, including formation of the clusters and the core-annulus structure. Useful information on cluster shapes, size, internal structure and core region size etc. has been collected (Li et al., 1980; Horio, 1994; Sharma et al., 2000; Lackermeier et al., 2001). Particularly, it has been found that the system instability is closely related to the properties of the fluid-particle system. Systems with large fluid-solid density difference more easily form clusters (Grace and Tuot, 1979).

However, owing to the complex and transient properties of dense gas-solid flows, the mechanism underlying the origin and evolution of the heterogeneous flow pattern have not been completely elucidated. Some researchers supposed that the core-annulus structure results from the wall effect, which slows down the gas phase and forms a swarm of particle clusters. However, there are indications (Hoomans, et al. 2000) that non-ideal particle-particle collisions cause formation of particle agglomerates and consequently lead to formation of a core-annulus flow structure. Furthermore, by employing discrete element simulation Helland et al. (2000) demonstrated that non-linear drag also leads to a heterogeneous flow structure.

In this paper, a computational study has been carried out to explore the mechanisms which control the cluster/dilute pattern formation by employing a discrete particle simulation approach (a "hard-sphere model" based on Molecular Dynamics). Particular attention was paid to the effect of 1) gas-solid interaction and 2) inelastic collisions between particles on pattern formation in high velocity gas-solid two-phase flows employing energy budget analysis to understand how the flow structures are related to these two phenomena. First, simulations were performed at conditions with different particle collisional properties to quantitatively understand collisional dissipation induced instability. Then, simulations with different gas phase properties (drag force), but zero collisional dissipation were carried out to explore the effect of gas-particle interaction on flow patterns. In addition, a system with strong collisional dissipation and enhanced gas-solid interaction (elevated pressure system) was studied to highlight whether there exists a necessary condition between those two instability-inducing factors by which the heterogeneous flow structure is initialized.

Theoretical background

In our discrete particle model the gas phase is described by the volume-averaged Navier-Stokes equation, whereas the particles are described by the Newtonian equations of motion while taking particle-particle and particle-wall collisions into account. The original computer codes for solving these sets of equations were developed by Kuipers (1992) for the gas phase and Hoomans (1999) for the granular dynamics including both 2D and 3D geometries. Additional codes were developed in this study to enable energy analysis.

Gas phase model

Continuity equation gas phase:

$$\frac{\partial(\varepsilon\rho_g)}{\partial t} + (\nabla \cdot \varepsilon\rho_g \boldsymbol{u}) = 0 \tag{1}$$

Momentum equation gas phase:

$$\frac{\partial(\varepsilon\rho_g \boldsymbol{u})}{\partial t} + (\nabla \cdot \varepsilon\rho_g \boldsymbol{u}\boldsymbol{u}) = -\varepsilon\nabla p - \boldsymbol{S_p} - (\nabla \cdot \varepsilon\bar{\boldsymbol{\delta}}_g) + \varepsilon\rho_g \boldsymbol{g} \tag{2}$$

where the source term S_p [Nm^{-3}] represents the reaction force to the drag force exerted on a particle per unit of volume suspension which is fed back to gas phase. In this work transient, two-dimensional, isothermal flow of air at atmospheric and elevated pressure conditions is considered.

Granular dynamics model

Force balance for a single particle:

$$m_p \frac{d\boldsymbol{V}}{dt} = m_p \boldsymbol{g} + \frac{V_p \beta}{1-\varepsilon}(\boldsymbol{u} - \boldsymbol{V}) - V_p \nabla p \tag{3}$$

In equation (3) the third term represents the force due to the pressure gradient. The second term is due to the drag force where β represents the interphase momentum

exchange coefficient similar to the one encountered in two-fluid models. The following well-known expression (Wen and Yu, 1970) has been used with $n = 2.7$.

$$\beta = \tfrac{3}{4} C_d \frac{\varepsilon(1-\varepsilon)}{d_p} \rho_g \left|\boldsymbol{u}-\boldsymbol{V}\right| \varepsilon^{-n} \tag{4}$$

The drag coefficient C_d is a function of the particle Reynolds number Re_p and given by:

$$C_d = \begin{cases} \dfrac{24}{Re_p}\left(1+0.15\, Re_p^{0.687}\right) & Re_p < 1000 \\ 0.44 & Re_p \geq 1000 \end{cases} \tag{5}$$

where Re_p is defined as:

$$Re_p = \frac{\varepsilon \rho_g \left|\boldsymbol{u}-\boldsymbol{V}\right| d_p}{\mu_g} \tag{6}$$

Simulation technology

The hard sphere model is used to describe a binary, instantaneous, inelastic collision with friction. The key parameters of the model are 1) the coefficient of restitution ($0<e<1$) and 2) the coefficient of friction ($\mu>0$). In this approach a sequence of binary collisions is processed. This implies that a collision list is compiled in which for each particle a collision partner and a corresponding collision time is stored. A constant time step is used to take the external forces into account and within this time step the prevailing collisions are processed sequentially. In order to reduce the required CPU time neighbour lists and cell lists are used. For each particle a list of neighboring particles is stored and only for the particles contained in this list a check for possible collision partners is performed. Validation of this simulation could be found in ref. (Hoomans et al., 2001). The simulations are carried out only for the central part of the riser section without considering inlet and exit effects. A certain amount of particles was fed at the bottom at a specified velocity according to a prescribed solid mass flux. When particles approach the top they are removed from the system. The simulation conditions are listed in Table 1. Effect due to particle size distribution are not included in this research, but can be found in Ref. (Hoomans et al., 2000).

Energy analysis

In fluid-particle systems, there exist two types of interactions: fluid-particle interaction due to drag and particle-particle interaction due to collisions. Our hard sphere based DPM model accounts for these two interactions in great detail and allows to compute the various work terms and energy types during the process. Thereby it is possible to study the underlying mechanisms, controlling flow pattern formation.

The particle phase energy analysis includes 1) energy input (work) to the particulate phase, which is composed of a) the work done by the drag force, b) system initial energy, c) energy introduced by newly fed particles; 2) energy budget distribution in the particulate phase, including kinetic, rotational, potential energies

and collisional dissipation. For circulating fluidized beds, the energy carried by outgoing particles should also be taken into account. According to the energy conservation principle for the particulate phase, the relationship between work done by drag and these energies is as follows:

$$W_{drg} = E_{dsp} + \Delta E_{pot} + \Delta E_{kin} + \Delta E_{rot} \tag{7}$$

For a circulating fluidized bed, we have:

$$W_{drg} = E_{dsp} + (E_{pot} + E_{pot,out}) + (E_{kin} + E_{kin,out}) + (E_{rot} + E_{rot,out}) - E_{inp,tot} - E^0_{tot} \tag{8}$$

where E^0_{tot} is the initial energy of the particulate phase and $E_{inp,tot}$ is the energy added by the feeding of particles at the inlet. In addition to the absolute energy, a parameter of the energy partition fraction was defined to characterize the energy budget:

$$f_i = \frac{E_i}{W_{drg} + E^0_{tot} + E_{inp,tot}} \tag{9}$$

where the subscript *i* refers to either total particle collisional dissipation, kinetic, rotational and potential energies respectively.

Results and discussions

Collisional dissipation induced instability

Figure 1(a) shows the snapshot of the flow patterns for e = 0.95, μ = 0.30. Compared to the flow pattern under conditions of ideal collisions (see Figure 1(b)), the case with non-ideal collisions produces a flow structure containing (dense) clusters. Also, the particle hold-up in the non-ideal case is higher than with ideal collisions. The energy budget analysis presented in Figure 2 clearly demonstrates that a higher portion of energy is consumed due to collisional dissipation, which greatly reduces both the particle potential and kinetic energy. This conclusion is similar to that drawn from a previous study on bubbling fluidized beds (Li and Kuipers, 2001). Once non-ideal particle-particle collisions prevail, a certain amount of energy is consumed due to the collisional dissipation. Particles have less energy to suspend themselves freely in space (raising potential energy). When new particles are encountered, additional dissipation occurs and the process repeats itself. If fluid-solid interaction is not strong enough to prevent the particles to approach each other, eventually a "particle cluster" is formed.

However, unlike the situation in dense gas-fluidized beds where particle clusters form as a continuous phase, all initial particle clusters in circulating fluidized beds can not connect each other to form a continuous emulsion phase, but only exist as individual separated "particle islands". This stems from the much stronger gas-solid interaction in CFB (potential energy fraction up to 80%, in Figure 2) compared to that in the dense bubbling beds (only 20%, Li and Kuipers, 2001). In other words, although collisional dissipation results in flow instability in both cases, owning to the fundamental change of particle-particle controlled interaction giving way to gas-solid controlled interaction, local heterogeneity is displayed in a circulating fluidized bed. For this mode of cluster formation mechanism, two conditions are necessary: one is the collision actually to occur and the other one is that the collisions should be

companied with energy dissipation. Should one of them not be fulfilled, a dissipation induced heterogeneous structure would be impossible. However, it should be noted that in Figure 2 some degree of flow heterogeneity still exists. What causes this heterogeneity then?

Non-linear gas drag induced instability

Many researchers have found from experiments that fluidization quality is closely related to the voidage exponent (2.35~4.7) in the well-known Richardson-Zaki (R-Z) equation: small values correspond to good fluidization quality or a uniform flow pattern. Unfortunately, a theoretical formulation to fully predict the drag force for such a dynamic system is still not available. Based on the R-Z correlation, Wen and Yu derived a drag correlation for a group of particles immersed in a fluid. In this well-known correlation a voidage exponent of 4.7 is employed. However, this fixed value is only valid in the high and low Reynolds number regime (Felice, 1994).

Figure 3 shows snapshots taken from the simulations with ideal collisions using the voidage exponents of 0 and 4.7 in the drag formulation respectively. Note that a value of n equal to 0 implies no effect of neighbour particles on the drag. Since this particle group effect on drag force is insensitive at low solid fraction, a higher solids flux of 75 kg/m^2.s has been employed in these simulations. In addition, the domain-averaged mean square solid volume fraction fluctuation, defined below, was used to quantitatively characterize and compare the flow structures.

$$< f_s'^2 >= \frac{1}{NR \cdot NZ} \sum_{j=1}^{NR \cdot NZ} (f_{s,j} - \bar{f}_s)^2 \qquad (10)$$

where NR, NZ are the number of computational cells in respectively the radial and axial direction and f_s is the solids volume fraction. The bar represents the domain-average. The results are shown in Figure 4. Clearly, particle clusters still exist in the system with ideal particle collisions. Our results indicate that a large voidage exponent produces a more uniform flow structure.

A comparison of the energy budget analysis for n = 0 and n = 4.7 focusing on the kinetic and potential energies (no dissipation and rotation due to ideal collision) is shown in Figure 5 indicating that the dominant drag force distributes a greater portion of the energy to particle motion. In addition, the domain-averaged granular temperature is shown in Figure 6 indicating that a bigger voidage exponent results in fewer collisions of particles. This means that the stronger group effect reduces the particle fluctuation motion and therefore the collision tendency. As a result, it results in a more homogeneous flow structure in circulating fluidized beds.

Combined effect of particle collision and gas drag

As shown above, both non-ideal particle-particle collision and non-linear drag could produce heterogeneous flow structures. However, the respective conditions and their induced cluster structures are different and therefore also a case was studied in which the combined effect of non-ideal particle-particle collision and a strong gas-solid interaction was considered.

Figure 7 shows the simulation results of run 4 with non-ideal particles at an elevated pressure of 50 bar and superficial gas velocity of 1.68 m/s (= 23u_{mf}), a strong "fluid-controlled" system. Clearly, we obtain a homogeneous flow structure. This

demonstrates that collisional dissipation can only play a role in case collisions can actually occur. In other words, it is not the necessary condition for heterogeneous flow structure formation. This could also be employed to explain the homogeneous flow patterns observed in most of the liquid/solid systems. Corresponding energy analysis, shown in Figure 8, indicates that nearly all energy is employed to suspend particles in such a case, implying that particles are always in an equilibrium state.

Different from cluster formation driven by collisional dissipation, the non-linear drag-induced cluster formation mechanism, which depends on the flow regime, material properties (viscosity, density and particle size), always plays a role if the drag force in the system has the non-linear voidage-dependent property. For circulating gas-fluidized beds operating at atmospheric conditions, owing to the large density difference, the non-linearity of the drag force always exists or particles are always in a non-equilibrium motion. Therefore, it is the fundamental source leading to particle agglomerate. Non-linear drag force has a "phase separation" function, which definitely enhances particle-particle collision. If the drag-force-induced particle collisions are non-ideal, it furthermore intensifies particle agglomeration.

Conclusions

Heterogeneous flow structures in circulating and collisonal fluidized beds could be induced by two kinds of mechanisms: non-linear drag force dissipation. For the simulated CFB system, smaller group effect in drag correlation produces a more pronounced heterogeneous flow pattern. Due to collisional dissipation particles consume energy drawn from gas phase up to 20%, which results in dense cluster formation. Between these two mechanisms, the non-linear drag force or gas-solid interaction is the key one resulting in heterogeneous flow structure formation. When both the non-linear drag and non-ideal particle collision take effect, a dense cluster/dilute flow structure is formed which finally leads to the core-annulus structure formation.

References

Felice R. D., "The Voidage Function for Fluid-Particle Interaction Systems", Int. J. of Multiphase Flow, 20, 153-159 (1994).

Grace, J. R. and J. Tuot, "A Theory for Cluster Formation in Vertically Conveyed Suspensions of Intermediate Density", Trans. Inst. Chem. Eng., 57, 49-54 (1979).

Helland, E., R. Occelli and L. Tadrist, "Numerical Study of Cluster Formation in a Gas-Particle Circulating Fluidized Bed", Powder Technology, 110, 210-221 (2000).

Hoomans, B. P. B., J. A. M. Kuipers and W. M. P. van Swaaij, "Discrete Particle Simulation of Cluster Formation in Dense Riser Flow", in "CFB-VI ", J. Werther, Ed., Wurzburg (1999), pp. 255-260.

Hoomans, B. P. B., J. A. M. Kuipers, W. P. M. van Swaaij, "Granular Dynamics Simulation of Segregation Phenomena in Bubbling Gas-Fluidized Beds", Powder Technology, 109, 41-48 (2000).

Hoomans, B. P. B., J. A. M. Kuipers, M. A. M. Salleh, M. Stein and J. P. K. Seville, "Experimental Validation of Granular Dynamics Simulations of Gas-Fluidised Beds with Homogenous in-Flow Conditions Using Positron Emission Particle Tracking, Powder Technology, 116, 166-177 (2001).

Horio, M. and H. Kuroki, "Three Dimension Flow Visualization of Dilutely Dispersed Solids in Bubbling and Circulating Fluidized Bed", Chem. Eng. Sci., 49, 2413-2421 (1994).

Kuipers, J. A. M., K. J. van Duin, F. P. H. van Beckum, and W. P. M. van Swaaij, "A Numerical Model of Gas-Fluidized Beds, Chem. Eng. Sci., 47, 1913-1924 (1992).

Lackermeier, U., C. Rudnick, J. Werther, B. Bredebusch, and H. Burkhardt, "Visualization of Flow Structures inside a Circulating Fluidized Bed by Means of Laser Sheet and Image Processing", Powder Technology, 114, 71-83 (2001).

Li, J. and J. A. M. Kuipers, "Effect of Pressure on Flow Behaviors in Dense Gas-fluidized Beds: A Discrete Particle Simulation Study", "Fluidization X", M. Kwauk, J. Li and W.-C. Yang, Eds., Engineering Foundation, Beijing (2001), pp.389-396

Li, Y. and M. Kwauk, "The Dynamics of Fast Fluidization", in: "Fluidization-III", J. R. Grace and J. M. Matsen, Eds., Plenum Press (1980), pp.537-544

Sharma, A. K., K. Tuzla, J. Matsen and J. C. Chen, "Parametric Effects of Particle Size and Gas Velocity on Cluster Characteristics in Fast Fluidized Beds", Powder Technology, 111, 114–122 (2000).

Wen, C.Y. and Y. H. Yu, "Mechanics of fluidization", Chem. Eng. Prog. Symp. Ser., 62, 100-111,(1966).

Table 1 Simulation conditions (for run1)

System	Bed height (m)	2	Width (m)	0.08
Particles	Density (kg/m^3)	2600	Diameter (μm)	500
	Solids flux (kg/m^{2}s)	25	Restitution coef. (e)	0.95
	Input vel. (m/s)	0.4	Friction coef. (μ)	0.30
Gas	Velocity (m/s)	5 (23u_{mf})	Pressure (bar)	1.20
Simulation	Grid	20 x100	dt (ms)	0.1
	Voidage exponent (n)	4.7		

Conditions for run 2: same as run1 except: e = 1.0, μ = 0; (run 2b: G_s = 75 kg/m^{2}s)
run 3: same as run 2 except: voidage exponent n = 0;
run 4: same as run 2 except: pressure 50 bar, U_g = 1.68 m/s (23 $u_{mf,50\ bar}$).

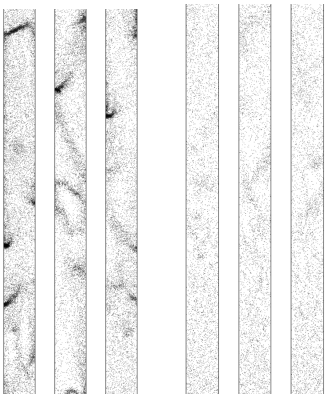

a) e=0.95, μ=0.3 b) e=1, μ=0

Figure 1. Flow structures in a CFB: *effect of collisional dissipation*.

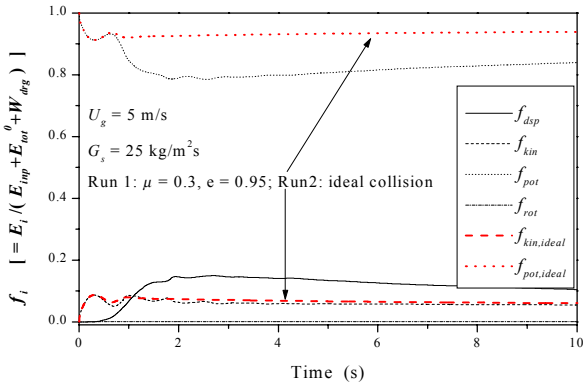

Figure 2. Energy analysis in circulating fluidized beds: collisional dissipated energy.

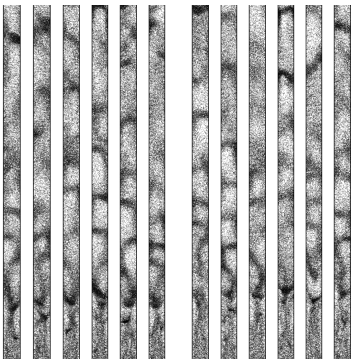

Figure 3. Flow structures in a CFB: *effect of non-linear drag,* (*ideal collisions,* $C_d = C_{d,single}.\varepsilon^{-n}$).

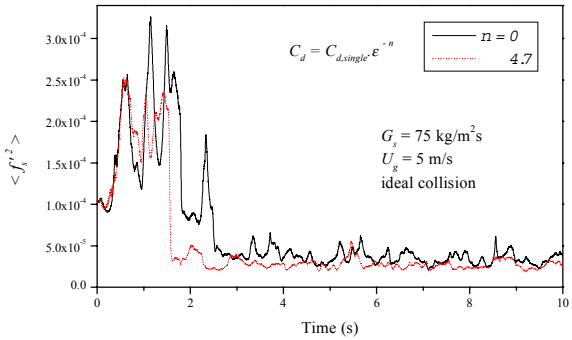

Figure 4. Domain-averaged mean square solids volume fraction fluctuation: *effect of exponent n.*

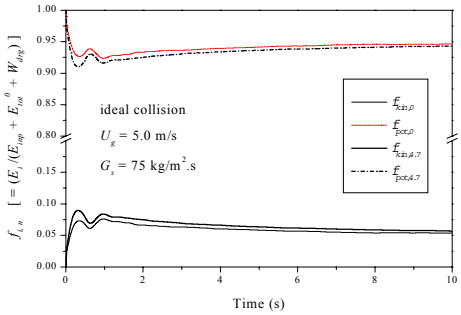

Figure 5. Energy analysis in circulating fluidized beds: *effect of nonlinear drag.*

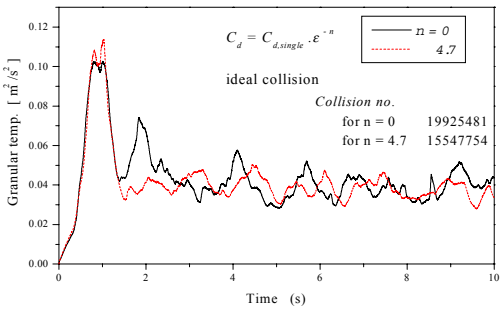

Figure 6. Granular temperature in CFB: *effect of nonlinear drag.*

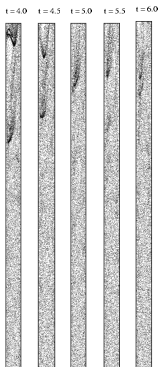

Figure 7. Flow structure in a CFB at elevated pressure (run 4): *homogeneous*.

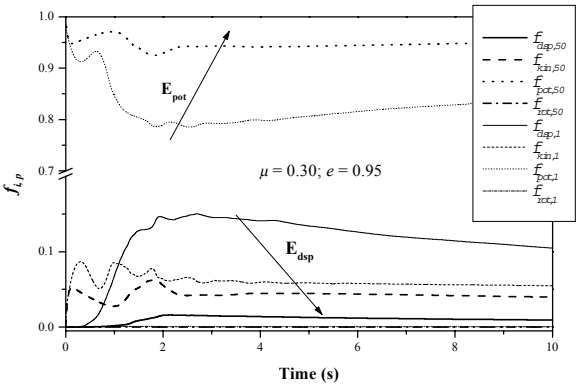

Figure 8. Comparison of energy budget analysis for the dissipation suppressed system at elevated pressure and the normal system at atmosphere pressure.